# Emittance Dilution due to Transverse Coupler Kicks in the Cornell ERL

Brandon Buckley, Joseph Choi, Georg H. Hoffstaetter
*Department of Physics, Cornell University, Ithaca, NY, 14853*
(Dated: June 3, 2006)

One of the main concerns in the design of a high energy Energy Recovery Linac x-ray source is the preservation of beam emittance. Discussed is one possible source of emittance dilution due to transverse electromagnetic fields in the accelerating cavities of the linac caused by the power coupler geometry. This has already been found to be a significant effect in Cornell's ERL injector cavities if only one coupler per cavity is chosen. Here we present results of simulations for Cornell's main ERL linac with three possible coupler configurations and compare them with regards to total normalized emittance growth after one complete loop through the linac. We have observed that the sign of the phase difference between the transverse kick and the accelerating force alternates each cavity. This leads to negligible emittance growth with a one-sided coupler configuration and non-negligible growth with an alternating coupler configuration. Only after optimizing the phase difference to zero do all configurations result in negligible emittance growth.

## I. INTRODUCTION

Cornell University is currently in the process of designing an Energy Recovery Linac (ERL) as a next generation x-ray source. As opposed to previous SR sources which store electrons for millions of turns in a storage ring, ERLs circulate electrons only once at very high energies and recover their energy to be used in the acceleration of new electrons. The proposed Cornell 5 GeV ERL contains two accelerating stages. The electrons are accelerated by two separate 2.5 GeV linacs connected by a non-accelerating return loop, then circulated through the Cornell Electron Storage Ring (CESR) and sent back into the linacs for energy recovery. In reusing the energy of electron bunches ERLs are capable of accelerating large currents at high energies at reasonable cost.

An imporant aspect of the electron beam, essential in the creation of highly focused x-rays, is the emittance. In order to create tightly focused radiation, the size and divergence of the electron bunches and thus the emittance must be small and must be maintained as the electrons are accelerated and circulated. The goal of the Cornell ERL is to have a normalized emittance increase of no more than 10%. The non-linearities in the accelerator causing emittance dilution must be studied and accounted for to satisfy this goal.

The ERL uses superconducting radio frequency (RF) cavities. Power couplers are placed near the entrance or exit of the cavities to supply an electric field in the longitudinal direction in order to accelerate the particles. It is advantageous to use only one coupler per cavity. However, due to this assymetric geometry the field close to the coupler is not rotationally symmetric about the cavity axis and produces a transverse kick on the electrons. This coupler kick varies as a function of time and thus, due to the finite length of an electron bunch, different parts of the bunch experience different kicks leading to emittance growth. As illustrated with similar studies dealing with the ERL's photoinjector, an approach that can be taken to reduce coupler kicks is decreasing the asymmetry in the coupler geometry

[1]. We have examined the effects due to three possible coupler configurations:

- Couplers all on one side
- Couplers alternating side every cavity
- Couplers alternating side every cryomodule, or every 10 cavities.

As a preliminary hypothesis one might guess that the emittance growth will vary monotonically with the symmetry in the coupler design. Hence, one would expect that alternating the couplers every cavity will have the least effect on emittance, followed by a configuration alternating the couplers every module, with a configuration keeping the couplers on the same side for every cavity causing the largest emittance growth.

We have also calculated the effects due to placing two couplers directly opposite each other at every cavity, eliminating the asymmetry and the transverse kick. Such a scenario would be very costly and thus one of the three configurations above would be preferred as long as the effects on the normalized emittance do not exceed the desired limit of 10% growth.

All results have been obtained running simulations with BMAD, a subroutine library developed at Cornell University by David Sagan et al. [2] designed to simulate the dynamics of relativistic charged particles through high energy accelerators and storage rings. A Gaussian distribution of 50000 electrons with initial normalized emittance of 100 nm in the x and y direction are sent through a lattice, hoff_erl05_07_27_3.lat, representing the ERL and CESR. The emittance at each element of the lattice is calculated and the results for the four proposed configurations are compared.

## II. CALCULATION OF ELECTROMAGNETIC FIELDS IN ACCELERATING CAVITIES AND THEIR COUPLER KICKS

BMAD makes it possible to simulate the effects of a coupler by inputing 4 paramaters: coupler_at, coupler_angle, coupler_strength, coupler_phase [2]. Coupler_at specifies whether the coupler is before or after the cavity. Coupler_angle is the direction with respect to the horizontal in which the kick is applied. For one-sided couplers this parameter is set to $90^\circ$ and for the other two configurations the alternate sided coupler has its coupler_angle set to $-90^\circ$. Coupler_strength is the transverse kick normalized to the energy gain in the cavity at the maximally accelerating phase, and coupler_phase is the phase of the transverse kick relative to this phase. These last two parameters are obtained through an in depth calculation of the coupler kick.

Firstly, the electromagnetic field inside the cavity due to the coupler must be calculated. This calculation is done utilizing CST Microwave Studios (MWS)[3], a software used for 3D electromagnetic field simulation of high frequency applications. A two cell model of the true seven cell RF cavity utilizing the Tesla gemoetry is inputed into the program(Fig. 1). Two separate calculations are run for two different boundary conditions at the end of the coupler: perfect electric wall and perfect magnetic wall. These boundary conditions are defined such that $\mathbf{E}^e = 0$ and $\mathbf{B}^m = 0$. In the coaxial coupler inward traveling waves are given by

$$\mathbf{E}^+ = \mathbf{e}_r \frac{A}{r}\cos(kz - \omega t + \varphi_0), \mathbf{B}^+ = \mathbf{e}_\varphi \frac{1}{c}\frac{A}{r}\cos(kz - \omega t + \varphi_0) \tag{1}$$

which can be verified by insertion into Maxwell's equations and checking the boundary conditions $\mathbf{E}_{||}(surface) = 0$ and $\mathbf{B}_{\perp}(surface) = 0$. An outward traveling wave has the form

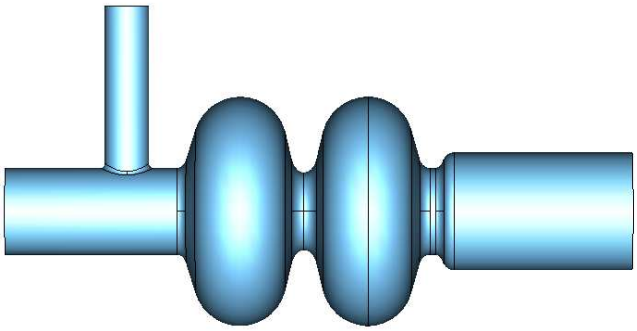

FIG. 1: A two cell MWS model of an ERL cavity utilizing Tesla geometry for the input coupler and the cell shape. A full ERL cavity contains 7 cells.

$$\mathbf{E}^- = \mathbf{e}_r \frac{A}{r}\cos(kz+\omega t+\varphi_0), \mathbf{B}^- = -\mathbf{e}_\varphi \frac{1}{c}\frac{A}{r}\cos(kz+\omega t+\varphi_0). \tag{2}$$

The standing wave patterns computed with MWS are superpositions of inward and outward traveling waves, $\mathbf{E}^e = \mathbf{E}^+ - \mathbf{E}^-, \mathbf{E}^m = \mathbf{E}^+ + \mathbf{E}^-, \mathbf{B}^e = \mathbf{B}^+ + \mathbf{B}^-, \mathbf{B}^m = \mathbf{B}^+ - \mathbf{B}^-$, with $\varphi_0 = 0$. In a coaxial coupler this means $\mathbf{E}^e = \mathbf{e}_r \frac{A}{r}\sin(kz)\sin(\omega t), \mathbf{E}^m = \mathbf{e}_r \frac{A}{r}\cos(kz)\cos(\omega t), \mathbf{B}^e = \mathbf{e}_\varphi \frac{1}{c}\frac{A}{r}\cos(kz)\cos(\omega t)$ and $\mathbf{B}^m = \mathbf{e}_\varphi \frac{1}{c}\frac{A}{r}\sin(kz)\sin(\omega t)$. MWS only computes the standing wave patterns $\hat{\mathbf{E}}^e, \hat{\mathbf{E}}^m, \hat{\mathbf{B}}^e$ and $\hat{\mathbf{B}}^m$ without time dependence so that $\mathbf{E}^e = \hat{\mathbf{E}}^e \sin(\omega t), \mathbf{E}^m = \hat{\mathbf{E}}^m \cos(\omega t), \mathbf{B}^e = \hat{\mathbf{B}}^e \cos(\omega t)$ and $\mathbf{B}^m = \hat{\mathbf{B}}^m \sin(\omega t)$. To make sure that the standing wave patterns computed with MWS have correct amplitudes we investigate them inside the coaxial coupler and we scale $\hat{\mathbf{B}}^e$ so that its amplitude is that of $\hat{\mathbf{E}}^m$ divided by c. Furthermore we adjust the signs of the standing waves computed with MWS such that they represent positive cosine and sine waves, taking the origin at the boundary of the coupler. After this normalization the two standing waves are combined via

$$\mathbf{E} = (\hat{\mathbf{E}}^m + i\hat{\mathbf{E}}^e)e^{-i\omega t}, \mathbf{B} = (\hat{\mathbf{B}}^e + i\hat{\mathbf{B}}^m)e^{-i\omega t} \tag{3}$$

to reconstitute a wave traveling down the coupler, $\mathbf{E}_{coupler} = \mathbf{e}_r \frac{A}{r} e^{i(kz-\omega t)}, \mathbf{B}_{coupler} = \mathbf{e}_\varphi \frac{1}{c}\frac{A}{r} e^{i(kz-\omega t)}$.

Using the Lorentz force law we can find the force on the electrons due to these electromagnetic fields,

$$\mathbf{F} = e(\mathbf{E} + \mathbf{v} \times \mathbf{B}), \tag{4}$$

and then can find the total change in momentum of an electron that travels along the central axis of the cavity with the speed of light

$$\triangle \mathbf{P} = e\int_{t_i}^{t_f} [\mathbf{E}(z,t) + c\mathbf{e}_z \times \mathbf{B}(z,t)]dt \tag{5}$$

with z = ct is a funtion of time. We can change our integration variable and rewrite Eq.(5) as

$$\triangle \mathbf{P} = \frac{e}{c}\int_0^L [\mathbf{E}(z, z/c) + c\mathbf{e}_z \times \mathbf{B}(z, z/c)]dz. \tag{6}$$

With the complex $\mathbf{E}$ and $\mathbf{B}$ of Eq.(3), $\triangle\mathbf{P}$ is a complex number of which only the real part is physical, $\triangle\mathbf{P}_{actual} = Re\{\triangle\mathbf{P}\} = |\triangle\mathbf{P}|\cos\phi$, where $\phi$ is the argument of $\triangle\mathbf{P}$. To better understand the dependence of $\phi$ we study the integral of Eq.(6).

Using the forms of $\mathbf{E}$ and $\mathbf{B}$ from Eq.(3) we can write $\triangle\mathbf{P}$ as

$$\triangle\mathbf{P} = \frac{e}{c}\int_0^L \{[\mathbf{E}^m(z) + i\mathbf{E}^e(z)] + c\mathbf{e}_z \times [\mathbf{B}^e(z) + i\mathbf{B}^m(z)]\}e^{-i\omega t(z)}dz. \tag{7}$$

For an electron arriving at z=0 at time $\triangle t = \frac{\triangle z}{c}$, $t(z) = \frac{z+\triangle z}{c}$. A time delay thus leads to a constant phase shift which we can remove from the integration

$$\triangle\mathbf{P}(\triangle z) = \triangle\mathbf{P}(0)e^{-i\frac{\omega}{c}\triangle z}. \tag{8}$$

From Eq.(8) it is clear that $|\triangle\mathbf{P}|$ is constant and the effect on $\triangle\mathbf{P}$ due to an offset of a particle by $\triangle z$ is merely a rotation in the complex plane, or a change of $-\frac{\omega}{c}\triangle z$ in the argument $\phi$ of $\triangle\mathbf{P}$. The actual change in momentum for an electron therefore depends on its position relative to the center of the bunch. It is exaclty this $\triangle z$ dependence that causes the emittance growth during acceleration, as electrons in different parts of the bunch will experience different kicks.

Another parameter affecting $\triangle\mathbf{P}$ is the placement of the coupler. In the ERL the position of the coupler alternates each cavity between the beginning and the end of the cavity. The fields obtained from the simulations run in MWS had the placement of the coupler at the beginning of the cavity. To model the fields induced by a coupler at the end of the cavity we use the same fields but take the mirror image and negate the $\mathbf{B}$ field,

$$\mathbf{E} = [\mathbf{E}^m(L-z) + i\mathbf{E}^e(L-z)]e^{-i\omega t}, \mathbf{B} = -[\mathbf{B}^e(L-z) + i\mathbf{B}^m(L-z)]e^{-i\omega t}. \tag{9}$$

To test if this truly describes the electromagneic fields inside the cavity with the coupler at the end we must determine if these fields represent a wave traveling down the coupler. If we take the mirror image of the fields inside the coupler, the $\mathbf{E}$ field, which is proportional to $\mathbf{e}_r$, will be unchanged. However, the $\mathbf{B}$ field which is proportional to $\mathbf{e}_\phi$ will have changed direction. Negating the $\mathbf{B}$ field in Eq.(9) reverses this change of direction. Since the original fields corresponded to an electromagnetic wave traveling down the coupler, with the double sign reversal the new fields will again correspond to an electromagnetic wave traveling down the coupler. With these new new fields we have

$$\triangle\mathbf{P} = \frac{e}{c}\int_0^L \{[\mathbf{E}^m(L-z)+i\mathbf{E}^e(L-z)]-c\mathbf{e}_z\times[\mathbf{B}^e(L-z)+i\mathbf{B}^m(L-z)]\}e^{-i\frac{\omega}{c}z}dz\cdot e^{-i\frac{\omega}{c}\triangle z}. \tag{10}$$

With a change of variable z=L-z we can rewrite this as

$$\triangle\mathbf{P} = \frac{e}{c}\int_0^L \{[\mathbf{E}^m(z) + i\mathbf{E}^e(z)] - c\mathbf{e}_z \times [\mathbf{B}^e(z) + i\mathbf{B}^m(z)]\}e^{i\frac{\omega}{c}z}dz \cdot e^{-i\frac{\omega}{c}(L+\triangle z)}. \tag{11}$$

Now we are able to define the coupler kick:

$$\kappa_y = \frac{\triangle P_y}{\triangle P_z} = \frac{|\triangle P_y|}{|\triangle P_z|}e^{i[\phi(\triangle P_y)-\phi(\triangle P_z)]} \tag{12}$$

and similarly for $\kappa_x$ where

$$\triangle P_y = \frac{e}{c}\int_0^L [E_y(z, z/c) + cB_x(z, z/c)]dz \tag{13}$$

and

$$\triangle P_z = \frac{e}{c}\int_0^L E_z dz. \tag{14}$$

MWS gives the magnetic field not as $\mathbf{B}$ but $\mathbf{H} = \frac{1}{\mu_0}\mathbf{B}$. Thus the magnetic force of Eq.(13) is calculated via

$$\triangle P_y^M = \frac{e}{c}\int_0^L (\frac{1}{\sqrt{\mu_0\epsilon_0}}\mu_0 H_x)dz = \mathbf{e}_y\frac{e}{c}\int_0^L (Z_0 H_x)dz. \tag{15}$$

Since the simulations in MWS were run with a 2 cell cavity, $\triangle\mathbf{P}_z$ of the actual 7 cell cavity has been taken as 3.5 times as large. It is assumed that $\phi(\kappa_x) = \phi(\kappa_y)$ which is satisfied whenever a cavity with a coupler has a symmetry plane. The parameters coupler_strength and coupler_phase inputed into the BMAD lattice describe these coupler kicks. Coupler_strength is defined as $\sqrt{|\kappa_x|^2 + |\kappa_y|^2}$. In our simulations we use a vertical coupler which prodcues $E_x$=0 and $B_y$=0 in the plane x=0 due to mirror symmetry in this plane. This leads to $\kappa_x = 0$ and coupler_strength= $|\kappa_y|$.

Coupler_phase is defined as $\phi(\kappa_y)$, the phase difference between $\triangle P_y$ and $\triangle P_z$. The coupler_phase is the phase of the coupler when the longitudinal kick is maximized, i.e. $\phi(\triangle P_z) = 0$. This phase is influenced by the distance the coupler is away from the beginning or end of the cavity.

## III. CALCULATION OF $Q_{ext}$

The external Q factor of a cavity is partially determined by the coupler geometry. We must therefore investigate which coupler geometry produces the required Q factor for the ERL cavities. Two possible values of $Q_{ext}$ for the ERL cavity that are studied are $Q_{ext} = 2 \times 10^7$ and $Q_{ext} = 1 \times 10^8$[4]. In the ERL cavity the important factor affecting the $Q_{ext}$ is the placement of the antenna inside the coupler. As illustrated in Fig. 2, the amount the antenna is lowered into the cavity can be varied and this parameter has a large effect on the external Q factor. In order to get an accurate simulation and realistic electromagnetic fields the depth of the antenna must be set appropriately.

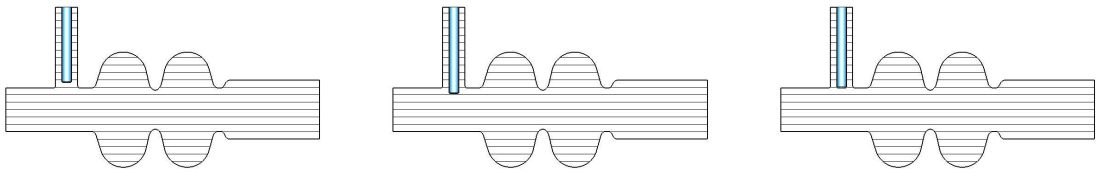

FIG. 2: A cross section of the ERL cavity illustrating varying depths of the coupler antenna.

Calculation of $Q_{ext}$ is carried out as follows, taking into account the energy loss in the coupler(for an in depth derivation see [5]),

$$Q_{ext} = Q_E + Q_H \tag{16}$$

where the quantities $Q_E$ and $Q_H$ are defined as

$$Q_E = \frac{2\omega UR}{V^2} \tag{17}$$

and

$$Q_H = \frac{2\omega U}{RI^2}. \tag{18}$$

$\omega$ is the frequency of the electromagnetic field, equal to 1.3 GHz, R is the impedance in the coaxial line, which in our case is equal to 50 ohms, and U is the energy stored in the cavity. This last quantity is set to 1 Joule due to the automatic normalization done by MWS when calculating the fields. The two parameters that are varied in the two equations are V and I which are, respectively, the voltage across the coaxial line and the current running along the line.

Multiple simulations were run in MWS for varying antenna depths and the fields taken at a radius of 15mm at the coupler boundary were used to calculate $Q_{ext}$. The results for a few values of depth can be found in table I. Depth values of -8.9mm and -16.24mm resulted in $Q_{ext}$ values of $2 \times 10^7$ and $1 \times 10^8$ respectively, and using the fields from these couplers we calculated the emittance growth.

TABLE I: The effects on $E$, $H$ and $Q_{ext}$ from varying antenna depth.

| depth(mm) | $E(\frac{C}{m})$ | $H(\frac{A}{m})$ | $Q_{ext}$ |
|---|---|---|---|
| 5 | $7.96\times10^4$ | 430 | $1.026\times10^6$ |
| 0 | $5.46\times10^4$ | 211 | $2.584\times10^6$ |
| -5 | $3.5\times10^4$ | 105 | $7.613\times10^6$ |
| -8.9 | $2.41\times10^4$ | 58 | $1.994\times10^7$ |
| -10 | $2.26\times10^4$ | 52.5 | $2.36\times10^7$ |
| -15 | $1.52\times10^4$ | 26.6 | $7.466\times10^7$ |
| -16.24 | $1.39\times10^4$ | 21.25 | $1.004\times10^8$ |

## IV. CLOSED ORBIT CORRECTIONS AND COUPLER PHASE MINIMIZATION

The cause of emittance dilution due to the coupler is the varying transverse kick along the bunch. However, there is also an overall transverse kick to the center of the bunch that causes an offset from the center of phase space. Due to sextupoles and other non-linearities in the return loop and CESR, this offset will lead to defocusing and even more emittance growth. Fortunately this is is easily corrected. Two corrector coils at the end of each cryomodule give two succesive kicks returning the center of the bunch back to the center of phase space. A program was written to calculate the necessary strengths of these kicks for each coupler configuration. The effects of the couplers and corrector coils on the orbit of one electron for the three coupler configurations with $Q_{ext} = 2 \times 10^7$ is illustrated in Fig. 3.

The emittance growth is minimized when the phase of the coupler kick for the center of the bunch is zero, as this leads to the smallest deviation in the transverse kick along the bunch. The effects of the coupler phase on emittance is illustrated in the following section.

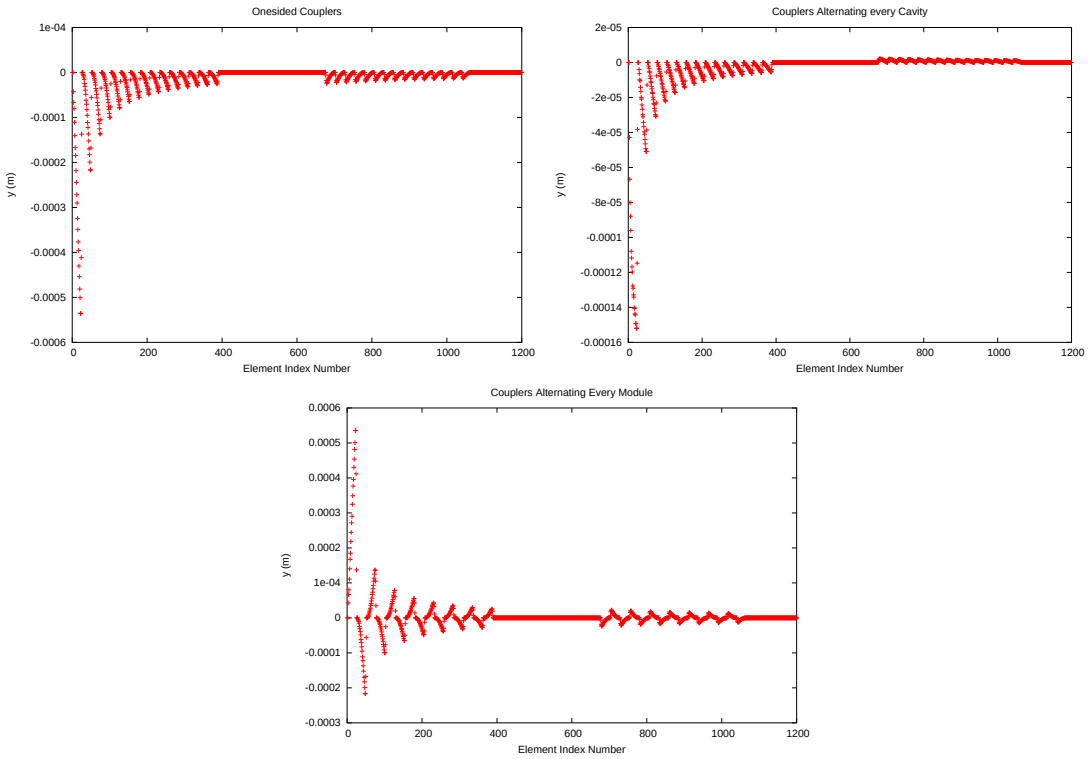


FIG. 3: Closed orbit of one electron through the two linacs and return loop with couplers and corrector coils.

## V. EMITTANCE GROWTH SIMULATIONS

With the above calculations completed, the coupler parameters were inputed into the hoff_erl05_07_27_3.lat BMAD lattice(Table II). Simulations were run with all four coupler scenarios for both $Q_{ext}$ values and the normalized emittance was calculated at every element of the lattice. The results are summarized in Figures 4 and 5.

TABLE II: Coupler Parameters Inputted into BMad prior to minimization of coupler_phase

| $Q_{ext}$ | Position of Coupler | coupler_strength | coupler_phase (rad/$2\pi$) |
|---|---|---|---|
| $2 \times 10^7$ | entrance | $1.0002857 \times 10^{-4}$ | .32307 |
| $2 \times 10^7$ | exit | $1.0022857 \times 10^{-4}$ | -.31351 |
| $1 \times 10^8$ | entrance | $1.00857 \times 10^{-4}$ | .321436 |
| $1 \times 10^8$ | exit | $1.0277143 \times 10^{-4}$ | -.31922 |

For one-sided couplers the emittance increases by less than 1.5%. When alternating coupler positions every cavity the emittance increases by a much larger value. Initially this might be surprising, but the coupler phase that approximately alternates from cavity to cavity compensates emittance growth in the first case and this effect is negated by alternating the coupler direcion in the second case.

To minimize the coupler phase this distance must be changed in the MWS simulations. Here we perform a simplified investigation. We do not change the coupler_strength but take as the optimal phase the average of the two coupler_phases from the couplers at the

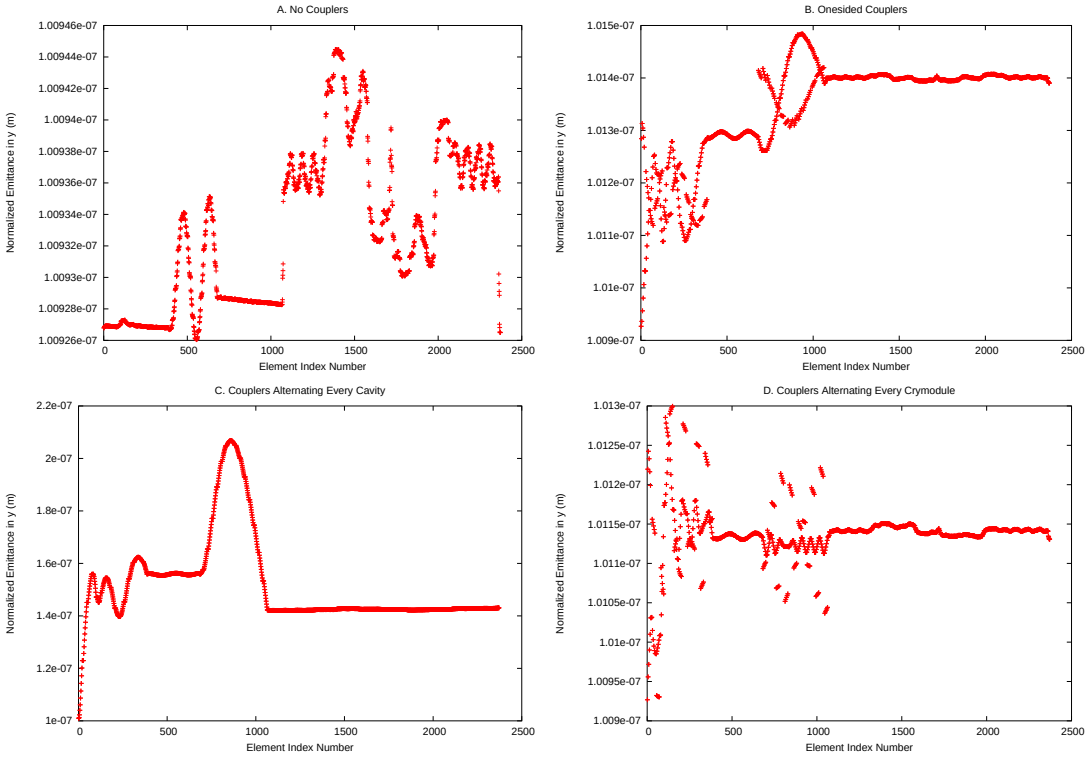


FIG. 4: Normalized emittance in the y direction for the three coupler configurations and without couplers for $Q_{ext} = 2 \times 10^7$.

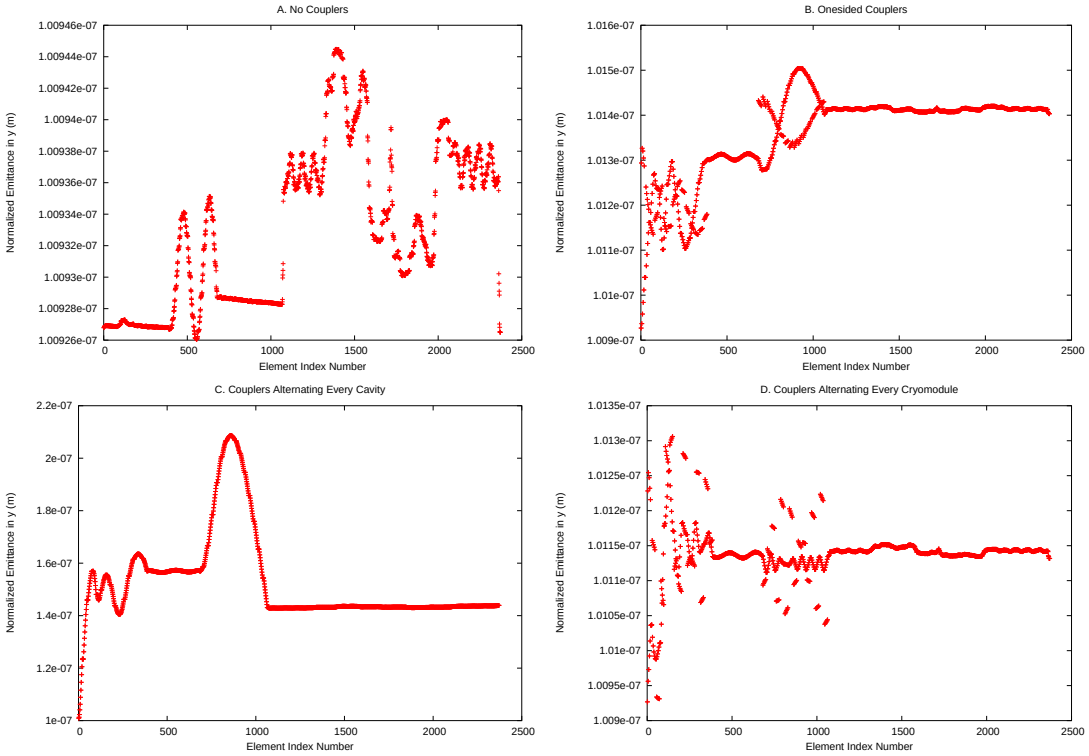


FIG. 5: Normalized emittance in the y direction for the three coupler configurations and without couplers for $Q_{ext} = 1 \times 10^8$.

beginning and the end of the cavity. The new coupler parameters can be found in Table III and the results in Figures 6 and 7. A summary of the emittance growth for all simulations can be found in Table IV.

TABLE III: Coupler Parameters Inputted into BMad after minimization of coupler_phase

| $Q_{ext}$ | Position of Coupler | coupler_strength | coupler_phase (rad/$2\pi$) |
|---|---|---|---|
| $2 \times 10^7$ | entrance | $1.0002857 \times 10^{-4}$ | .004780 |
| $2 \times 10^7$ | exit | $1.0022857 \times 10^{-4}$ | .004780 |
| $1 \times 10^8$ | entrance | $1.00857 \times 10^{-4}$ | .001108 |
| $1 \times 10^8$ | exit | $1.0277143 \times 10^{-4}$ | .001108 |

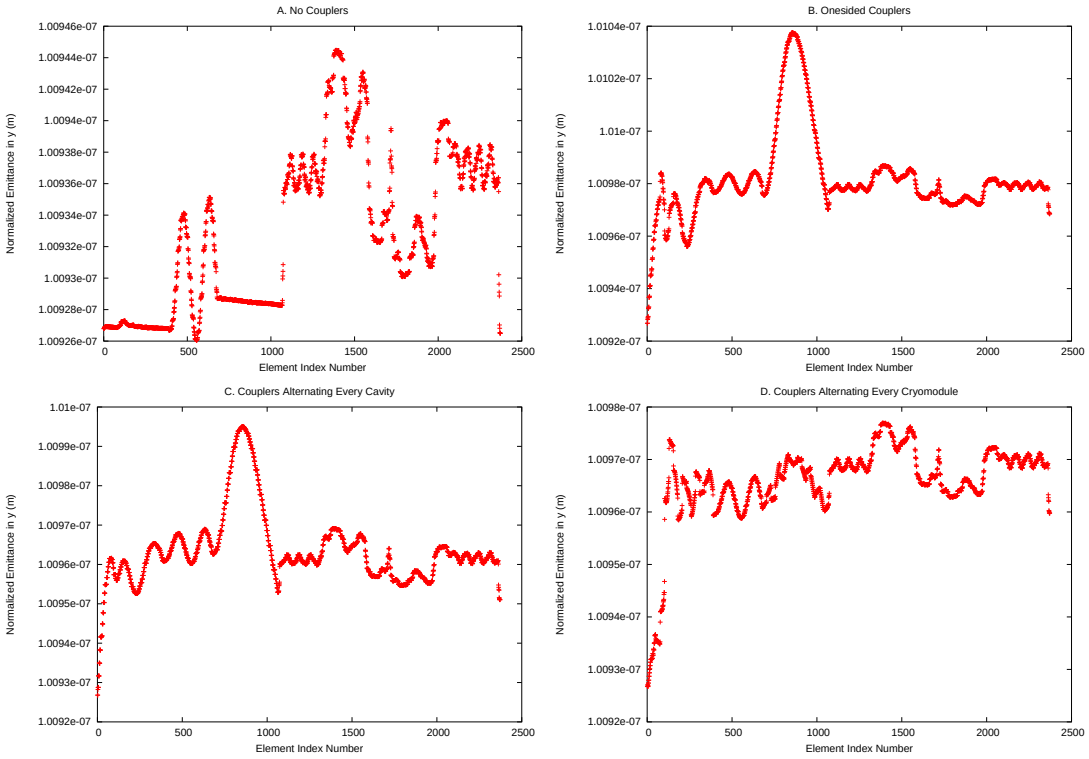


FIG. 6: Normalized emittance in the y direction for the three coupler configurations and without couplers for $Q_{ext} = 2 \times 10^7$ with minimized coupler_phase.

## VI. CONCLUSION

These results illustrate the importance of the phase of the coupler kick. Prior to minimzation of the coupler_phase emittance growth is non-negligible with alternating the coupler orientation every cavity while negligible with the other two configurations. After minimization of coupler_phase emittance growth is negligible with all configurations. Incidentally, after minimization our initial hypothesis is satisfied and the emittance growth is minimal when alternating the coupler orientation every cavity. This is due to the fact that the

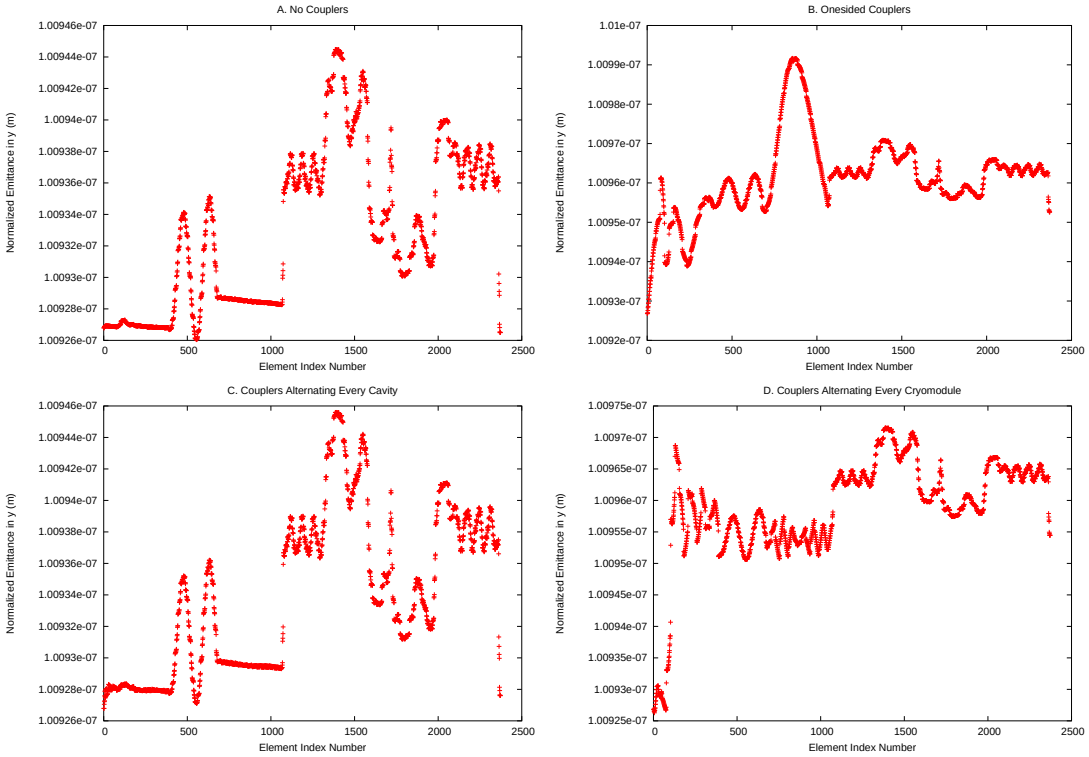


FIG. 7: Normalized emittance in the y direction for the three coupler configurations and without couplers for $Q_{ext} = 1 \times 10^8$ with minimized coupler_phase.

TABLE IV: Percentage Increase of Emittance Growth for All Configurations

| | Phase not minimized | | Phase minimized | |
|---|---|---|---|---|
| | $Q_{ext} = 2 \times 10^7$ | $Q_{ext} = 1 \times 10^8$ | $Q_{ext} = 2 \times 10^7$ | $Q_{ext} = 1 \times 10^8$ |
| No Couplers | 0.9% | 0.9% | 0.9% | 0.9% |
| Onesided | 1.39% | 1.40% | 0.97% | 0.95% |
| Alternating Cavities | 43.07% | 43.92% | 0.95% | 0.93% |
| Alternating Cryomodules | 1.13% | 1.13% | 0.96% | 0.95% |

coupler_phases no longer alternate sign. Since the one-sided coupler arrangement is technically most feasible, and since it leads to tolerable emittance growth even for non-optimized coupler phases, we propose to use this arrangement for the Cornell x-ray ERL. For such an arrangement, without optimized coupler phases, it is essential for the coupler position to alternate from before and after the cavities.

[1] V. Shemelin et. al., *Low-Kick Twin-Coaxial and Waveguide-Coaxial Couplers for ERL*, Cornell Universtiy LNS report SRF 021028-08 (2002)
[2] D. Sagan, *BMad Manual*, http://www.lns.cornell.edu/ dcs/bmad/ (2006)
[3] CST Microwave Studio, User Guide, CST GmbH, Budinger Str. D-64289 Darmstadt, Germany
[4] M. Liepe et. al., *Pushing the Limits: RF Field Control at High Loaded Q*, Proceedings of the

2005 Particle Accelerator Conference, Knoxville, TN, USA (2005)

[5] V. Shemelin et. al., *Calculation of the B-cell cavity external Q with MAFIA and Microwave Studios*, Cornell University LNS report SRF 020620-03 (2002)